

On geometry dependent R -curve from size effect law for concrete-like quasibrittle materials

Yan-hua Zhao^{*}, Jian-mei Chang^{1,2} and Hong-bo Gao³

¹State Key Laboratory of Coastal and Offshore Engineering,
Dalian University of Technology, Dalian, China 116024

²Transportation Institute, Inner Mongolia University, Hohhot, China 010070

³College of Civil Engineering and Architecture, Hainan University, Haikou, China 570228

(Received July 21, 2014, Revised October 4, 2014, Accepted November 15, 2014)

Abstract. R -curve based on the size effect law previously developed for geometrically similar specimens (geometry type III) is extended to geometries with variable depth (geometry type I) as well as with variable notch (geometry type II), where the R -curve is defined as the envelope of the family of critical strain energy release rates from specimens of different sizes. The results show that the extended R -curve for type I tends to be the same for different specimen configurations, while it is greatly dependent on specimen geometry in terms of the initial crack length. Furthermore, the predicted load-deflection responses from the suggested R -curve are found to agree well with the testing results on concrete and rock materials. Besides, maximum loads for type II specimen are predicted well from the extended R -curve.

Keywords: fracture mechanics; size effect law; energy release rate; R -curve

1. Introduction

Within the framework of fracture mechanics, R is often used to denote the crack resistance, meaning the amount of energy needed to grow a pre-existing crack. For quasi-brittle materials such as concrete, ceramic, rock and wood, a more or less pronounced rising R -curve is common due to the existence of a sizable fracture process zone (FPZ) at the crack front which may consume a large amount of energy during crack growth (Bažant *et al.* 1986, Ferreira *et al.* 2002, de Moura *et al.* 2008, Xu and Zhang 2008, Kumar and Barai 2009, de Moura *et al.* 2010, Xu *et al.* 2011, Dong *et al.* 2013). R -curve approach has been successfully used to predict the structure response, i.e., the maximum load, load-displacement (or load-crack mouth opening displacement) as well as other material fracture properties. In all, the R -curve may provide a deeper physical insight into the material fracture. For that purpose, many attempts have been made to find a solution for the R -curve described by the variation of fracture energy versus the crack extension. One direct way is to evaluate the critical energy release rate from the load-deflection curve, which may require an accurate measurement or definition of the crack extension length or the concept of “the effective crack length” (Jenq and Shah 1985a, Morel *et al.* 2008). R -curve results in this way are limited due to the difficulty or ambiguity in experimental location of the crack tip especially for quasi-brittle

*Corresponding author, Associate Professor, Ph.D., E-mail: yanhuazh@dlut.edu.cn

materials. Alternatively, the idea that the R -curve is a unique function of the crack extension originated for metals (Krafft *et al.* 1961) has been borrowed to derive an analytical solution of R -curve based on different fracture models. Fig.1 shows three typical geometrical configurations frequently used to study fracture behavior in materials. Accordingly three types of R -curve were defined according to the different geometrical size (Ouyang *et al.* 1990).

(i) type I for constant a_0 and changeable d , where R -curve is defined as an envelope of the energy release rates with different specimen size d but the same initial notch length a_0 . By assuming that the critical crack length is proportional to the initial crack length, a formulation of R -curve was proposed by solving an Euler equation (Ouyang *et al.* 1990, Ouyang and Shah 1991). Two necessary parameters for this formulation, the critical stress intensity factor (K_{Ic}^s) and the critical crack tip opening displacement ($CTOD_c$), two fracture parameters defined in the two parameter fracture model (TPFM) can be determined according to the RILEM recommendation (RILEM 1990).

(ii) type II for the same specimen depth d and different initial crack length a_0 . For this situation, R -curve is defined as an envelope of the energy release rates with different a_0 but the same specimen size. A general expression for R -curve was obtained in (Yang and Shah 2001), which is also based on the hypothesis that the critical crack length is proportional to the initial crack length.

(iii) type III for specimen by changing a_0 and d proportionally. R -curve for this type is defined as an envelope of the energy release rates for a set of geometrically similar specimens. The R -curve developed by Bažant (Bažant and Kazemi 1990) falls into type III, since its underlying idea is based on the size effect law (SEL) for geometrically similar specimens. The R -curve in type III specimen depends on two material fracture parameters, that is, G_f and c_f , meaning the critical energy release rate and crack extension in an infinitely large specimen. By definition, G_f and c_f should be independent of specimen size and specimen shape and therefore can be regarded as material properties. RILEM recommended in 1991 to determine G_f and c_f (RILEM 1991).

The generalized SEL permits the use of specimens not only of geometrically similar size (type III) but also of variable-notch one size (Tang *et al.* 1996). In other words, R -curve for specimen type II can be theoretically derived based on SEL. For type I, the initial crack length a_0 is believed to be a material characteristic length thus the study on R -curve for type I may be more of a practical use. The present paper has the objective of verifying the feasibility of SEL to R -curve for type I and type II with highlight on type I. Simultaneously, geometry dependence of R -curve is investigated to give a deeper understanding of the nature of R -curve. To avoid complexity, we restrict our investigation to fracture under mode I.

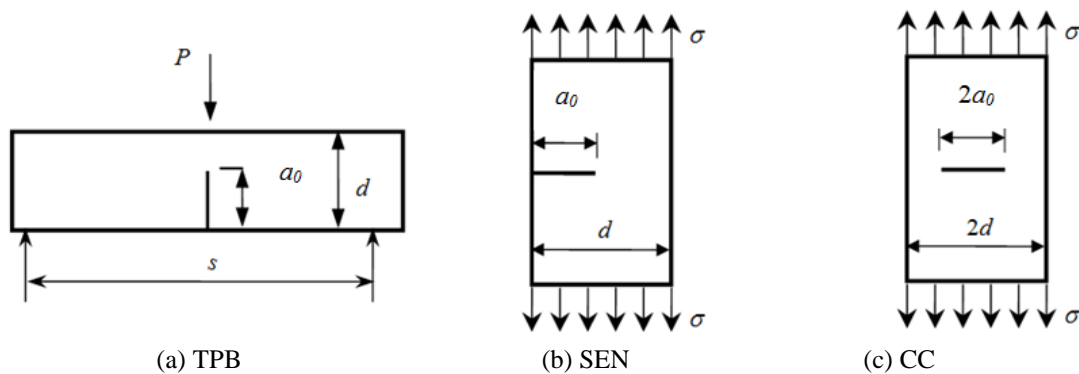


Fig.1 Specimen geometries for R -curve determination

2. General rule to construct R-curve

For a three-point-bending beam (TPB) shown in Fig.1(a), the nominal strength at failure can be described

$$\sigma_N = c_n \frac{P_u}{td} \quad (1)$$

where P_u is the maximum load, $c_n = 1.5s/d$ is a coefficient introduced for convenience, and t is the thickness of the specimen.

The critical energy release rate when the load attains its peak value P_u can be written based on the theory of linear elastic fracture mechanics (LEFM)

$$G(a) = \frac{P_u^2}{Et^2d} g(\alpha) \quad (2)$$

where E is the elastic modulus, and $g(\alpha)$ is a certain non-dimensional function of the relative crack length $\alpha = a/d$ characterizing the shape of the structures.

The generalized SEL can be rewritten in the following form (Bažant and Kazemi 1990)

$$\sigma_N = c_n \left(\frac{EG_f}{g'(\alpha_0)c_f + dg(\alpha_0)} \right)^{1/2} \quad (3)$$

where $\alpha_0 = a_0/d$, and $g'(\alpha_0)$ is the first derivative of $g(\alpha)$ with respect to α when $\alpha = \alpha_0$. Two crucial parameters in the generalized SEL are G_f and c_f . By definition, these two parameters are theoretically material-related only.

When the stress intensity factor at the crack tip is put in a typical form

$$K_I = \sigma \sqrt{\pi a} g_1(\alpha) \quad (4)$$

Then $g(\alpha)$ in Eq.(2) is related to $g_1(\alpha)$ by

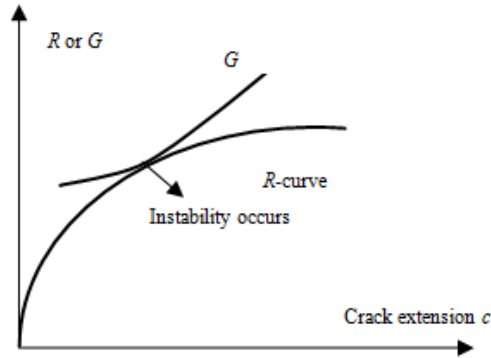
$$g(\alpha) = \pi \alpha c_n^2 g_1^2(\alpha) \quad (5)$$

For many typical specimen geometries, the values of $g_1(\alpha)$ in the Eqs.(4)-(5) can be found in the handbook [Tada *et al.* 2000].

Substitution of Eq.(1) and Eq.(3) into Eq.(2) yields the equation of the critical energy release rate for TPB specimens

$$\frac{G(a)}{G_f} = \frac{dg(\alpha)}{g'(\alpha_0)c_f + dg(\alpha_0)} \quad (6)$$

For concrete and rock like quasi-brittle materials, instability is often preceded by a certain amount of slow crack growth which leads to a rising R-curve behavior. R-curve is generally treated as a function of crack extension c , i.e., $R(c)$. To ensure instability occurs, two conditions must be satisfied (c.f. Fig.2)

Fig. 2 Definition of R -curve

$$G(a) = R(c) \quad (7a)$$

$$\frac{\partial G(a)}{\partial a} = \frac{\partial R(c)}{\partial c} \quad (7b)$$

Eqs. (7a)-(7b) indicate that R -curve can be regarded as the envelope of the critical energy release rates from specimens of different size, and it holds true for geometry type I, type II and type III, which gives us a hint to construct R -curve analytically. Mathematically speaking, R -curve can be developed by setting equal to 0 the partial derivative of Eq.(7a) with respect to the parameter involved. Though for different geometry type, different parameter is concerned. R -curve defined by Eqs. (7a)-(7b) is in all governed by two geometrical factors, a_0 and d . Specifically, for type I since a_0 is fixed, d is the only parameter; for type II, d is constant and R -curve is a parameter equation with respect to a_0 ; while for type III, a_0/d keeps unchanged, a_0 or d could be regard as the parameter influencing the R -curve. Detailed discussions are presented in the following sections.

3. R -curve for geometry type I

For geometry type I, only specimen size d is the variable, and a_0 is fixed. To calculate R -curve, a series of c values in terms of c/c_f is chosen, and for each c/c_f the value of d is solved from Eq.(6) by setting $\frac{\partial G}{\partial d} = 0$. Then R -curve is constructed by substituting d solved and $\alpha = (a_0 + c)/d$ into Eq.(7a). Note c/c_f , the coordinate for R -curve should be less than one unit when the above calculation is proceeded, since for $c/c_f \geq 1$, $R = G_f$.

When $R(c)$ is known in advance, fracture response of a specimen, such as load-displacement may be predicted by the following simple algorithm.

(i) Assign a small crack increment c and set $a = a_0 + c$, where a is considered to be an equivalent elastic crack.

(ii) For each c calculate $R(c)$. For crack a to grow, $G(a)$ should be equal to $R(c)$. Using LEFM,

the load corresponding to a can be calculated based on the following equation

$$R(c) = G(a) = \frac{P^2}{Et^2d} g(\alpha) \quad (8)$$

(iii) For each $a=a_0+c$ and its corresponding load P above, the total load-line displacement δ_{tol} can be obtained using

$$\delta_{tol} = \delta_0 + \delta_{crack} \quad (9)$$

where δ_0 responds to displacement caused by load P in the same specimen without crack and for bending situation

$$\delta_0 = \frac{Ps^3}{4Etd^3} \quad (10)$$

δ_{crack} is the additional load point displacement due to the existence of crack (Tada *et al.* 2000)

$$\delta_{crack} = \frac{3PS^2}{2Etd^2} V(\alpha) \quad (11)$$

For $s/d=4$

$$V(\alpha) = \left(\frac{\alpha}{1-\alpha} \right)^2 (5.58 - 19.57\alpha + 36.82\alpha^2 - 34.94\alpha^3 + 12.77\alpha^4) \quad (12)$$

The above formula has better than 1% accuracy for any α .

(iv) Repeat (i)-(iii) until the load P approaches zero.

The experimental results (Bažant *et al.* 1991, Jenq and Shah 1985b) on rock and concrete are used to testify the proposed R-curve approach. Necessary test results on Indiana limestone for different size are illustrated in Table 1.

For TPB with $s/d=4$, c_n in Eq.(1) equals to 6 and $g_1(\alpha)$ in Eq.(5) has the form (Tada *et.al* 2000)

$$g_1(\alpha) = \frac{1.99 - \alpha(1-\alpha)(2.15 - 3.93\alpha + 2.70\alpha^2)}{\sqrt{\pi}(1+2\alpha)(1-\alpha)^{3/2}} \quad (13)$$

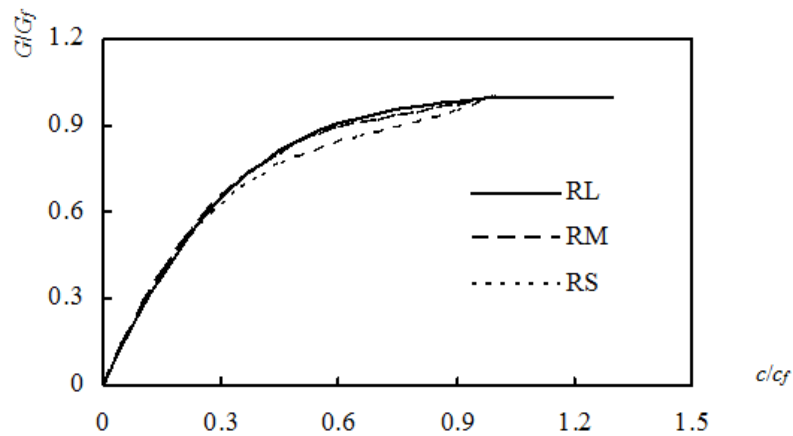
Eq.(13) has an accuracy 0.5% for any α .

Fig.3 plots R-curves for three specimens of rock determined using the proposed method. Rising behavior of R-curve is well depicted which is attributed to the energy consumption of FPZ. For further investigation, an explicit expression for R-curve may be easier for programming. The following formula fitted by means of software Excel appears to work well with the coefficient of determination R square close to 1.

Table 1 Rock test results reported in (Bažant *et al.* 1991)

Specimen label	Dimensions(mm) ($s \times d \times t \times a_0$)	Peak load (N)	G_f (N/mm)	c_f (mm)	E (MPa)
RL	457×102×13×41	418, 405, 394 (406)*			
RM	229×51×13×21	238, 243, 243 (241)*	0.061	9.3	15300
RS	114×25×13×10	134, 140, 140 (138)*			

* Note: value in the parenthesis is the average

Fig. 3 R -curves for rock material of different a_0 Table 2 β_1 , β_2 , and β_3 for rock of different size

	β_1	β_2	β_3
RL	1.2168	-3.2323	3.0155
RM	1.4976	-3.5975	3.0999
RS	1.8812	-3.9743	3.0931

$$\begin{cases} \frac{R(c)}{G_f} = \beta_1 \left(\frac{c}{c_f}\right)^3 + \beta_2 \left(\frac{c}{c_f}\right)^2 + \beta_3 \left(\frac{c}{c_f}\right), & \frac{c}{c_f} \leq 1 \\ \frac{R(c)}{G_f} = 1, & \frac{c}{c_f} > 1 \end{cases} \quad (14)$$

where β_1 , β_2 , and β_3 are coefficients for better fitting and their values for different size rock specimens are tabulated in Table 2.

With R -curve known, the theoretical load-displacement relation could be easily predicted using

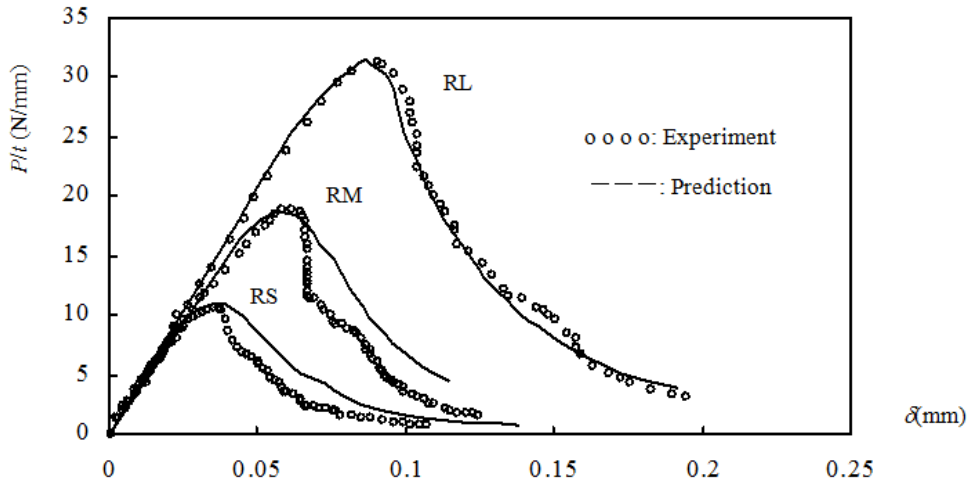


Fig.4 Comparison of experimental and theoretical results for rock

Table 3 Mechanical parameters corresponding to Point C and Point F

	Point C			Point F			
	$P_u(N)$	$a_u(mm)$	$c_u(mm)$	$P_f(N)$	$a_f(mm)$	$c_f(mm)$	$CTOD_f(mm)$
RL	400.65	46.4	5.4	375.98	50.3		0.034
RM	238.08	24.9	3.9	187.84	30.3	9.3	0.024
RS	138.99	12.4	2.4	54.72	19.3		0.021

the procedure described earlier and Fig.4 shows the comparison between the theoretical solution and experimental result and a favorable agreement is observed.

During computation, R value for specimen of a finite size is not assumed to be a plateau value after the load attains its peak value P_u . From our study, FPZ has not gained its fully development when the load reaches its maximum value (Zhao *et al.* 2007), and the energy dissipating in the FPZ continues to grow until FPZ evolves fully and begins to detach from the crack tip and advances ahead with an approximate same size and thus the same amount of energy. A simple possible explanation is sketched in Fig.5, where Point C and F denote the peak load and the onset of propagation at constant fracture resistance G_f respectively. The load, equivalent crack length and equivalent crack extension for Point C and F are represented by P_u , a_u , c_u and P_f , a_f , c_f respectively, where $c_u = a_u - a_0$ and $c_f = a_f - a_0$. According to the R -curve approach, these values could be easily obtained except that $c_f = 9.3mm$ is already known for the limestone under consideration, and the obtained results are given in Table 3.

At the Point C, the maximum load P_u from the proposed R -curve approach is very close to the experimental measurement in Table 1. Also at the Point C FPZ has not gained its fully development and the cohesive force at the original crack tip is not assumed to be zero shown in Fig.5(b). At the Point F, FPZ reaches its fully evolution after which FPZ may detach from the

original crack tip and start to grow forward with the fixed length, and the energy needed will stay unchanged as G_f . At this moment the cohesive force at a_0 is supposed to be zero marking the detachment shown in Fig.5(c). By substituting the related parameters listed in Table 3 into the following two empirical expressions (Jenq and Shah 1985b), crack tip opening displacement ($CTOD$) at Point F can be obtained and the computation results are also listed in Table 3.

$$\frac{CTOD_f}{CMOD_f} = \left\{ \left(1 - \frac{a_0}{a_f}\right)^2 + (1.081 - 1.149 \frac{a_f}{d}) \left(\frac{a_0}{a_f} - \left(\frac{a_0}{a_f}\right)^2\right) \right\}^{1/2} \tag{15a}$$

$$CMOD_f = \frac{6P_f s a_f}{d^2 t E} V_1(\alpha_f), \alpha_f = \frac{a_f}{d} \tag{15b}$$

where
$$V_1(\alpha_f) = 0.76 - 2.28\alpha_f + 3.87\alpha_f^2 - 2.04\alpha_f^3 + \frac{0.66}{(1 - \alpha_f)^2} \tag{15c}$$

Eq.(15b) is within 1% accuracy and $V_1(\alpha)$ is valid for $s/d=4$.

A simple linear softening relation is taken for our example, and the crack opening displacement for complete fracture is taken to be $2G_f / f_t = 2 \times 0.061 / 5 = 0.0244\text{mm}$ where $f_t=5\text{MPa}$ is the tensile strength reported in (Bažant *et al.* 1991), and this value is close to the predicted value $CTOD_f$ in Table 3, which confirms our previous assumption that the R -curve is still increasing after the peak load until FPZ gains its fully development and then leveling off of the R -curve indicates FPZ will evolve at a steady state. A similar phenomenon has also been detected in the tests on the wood material (Ferreira *et al.* 2002, de Morel *et al.* 2010).

The size of the concrete beam in (Jenq and Shah 1985b) were $305 \times 76 \times 29 \times 22(\text{mm}) (s \times d \times t \times a_0)$, and the Young's modulus for elasticity $E=20000\text{MPa}$ was chosen for a better match with the

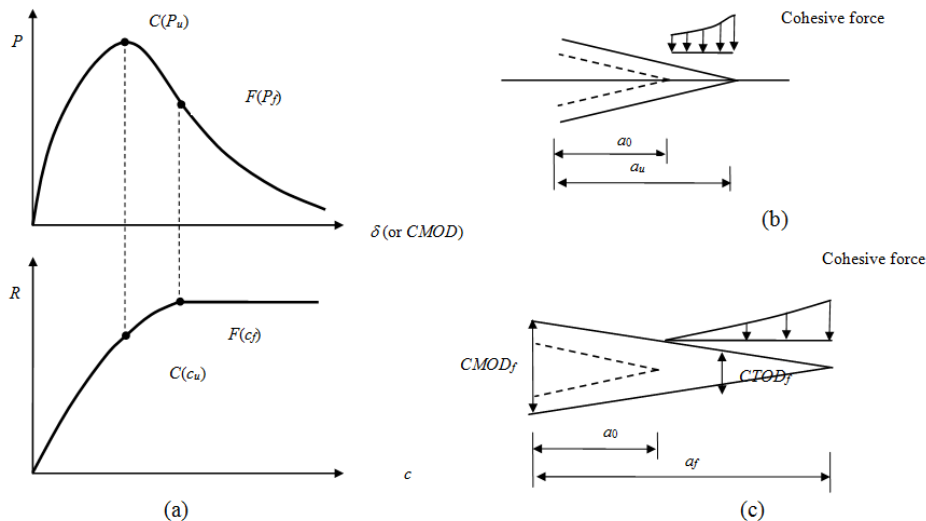


Fig.5 Description of leveling off of R-curve

experimental initial compliance of $P-\delta$ curve. Two prerequisite parameters for the R-curve model, i.e., G_f and c_f can not be extracted from the test results directly and only K_{Ic}^s and $CTOD_c$ were provided in the test. Since these two pairs are assumed to be materials properties, their equivalency can be established from the infinitely large TPB specimen based on LEFM

$$G_f = \frac{K_{Ic}^s}{E} \tag{16a}$$

$$c_f = -0.5405a_0 + 0.0545A + \sqrt{0.292a_0^2 + 0.05a_0A + 0.00297A^2}, \quad A = \frac{CTOD_c^2 E}{G_f} \tag{16b}$$

Inserting the average values $K_{Ic}^s = 31.45\text{N/mm}^{3/2}$ and $CTOD_c = 0.02\text{mm}$ leads to $G_f = 0.0492\text{N/mm}$ and $c_f = 16.94\text{mm}$. With these two parameters known, the same procedure as in rock is conducted and the $P-\delta$ curve for this specimen is evaluated, and Fig.6 gives its comparison with the experimental recording.

Fig.6 implies that the global response of the specimen can be well simulated by the proposed R-curve model, though the maximum load P/t from the R-curve approach is 31.34N/mm , a little higher than the four peak load values 29.62N/mm , 24.55N/mm , 27.31N/mm and 30.47N/mm . Next R-curve geometry-dependence is explored by changing a_0 and specimen geometry configuration. $G_f = 0.0492\text{N/mm}$ and $c_f = 16.94\text{mm}$ from the above concrete test are utilized for this purpose. a_0 are chosen to be 10mm , 15mm and 22mm , and the geometries for study are TPB, single edge notch (SEN) and center cracked specimen (CC). These three geometries are shown in Fig.1. For different geometries, c_n and $g_1(\alpha)$ have different expressions (Tada *et al.* 2000)

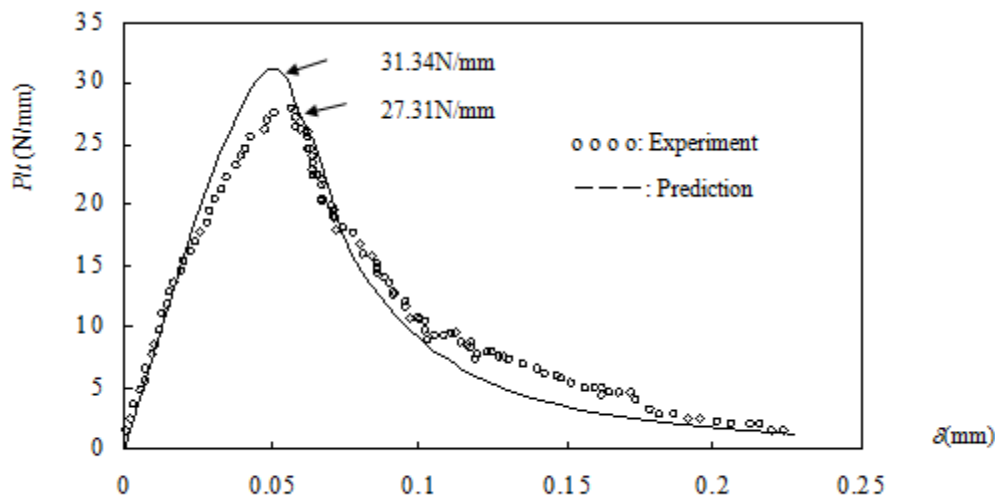
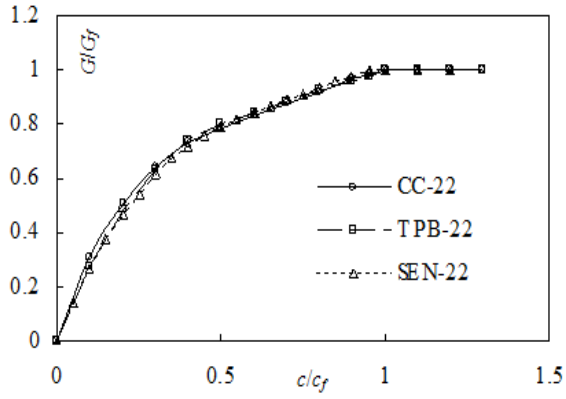
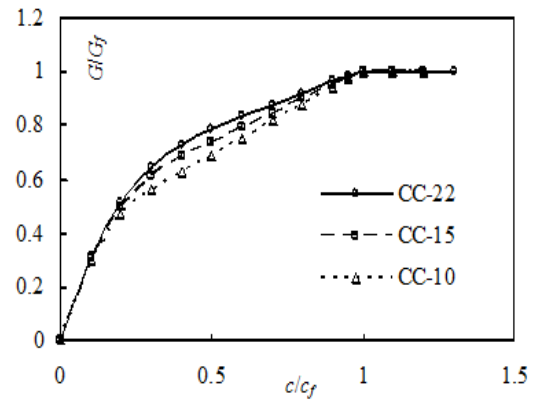


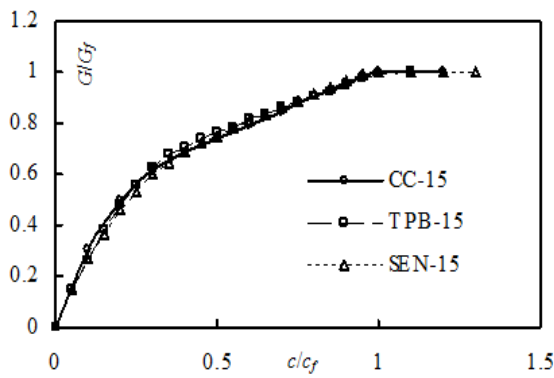
Fig.6 Comparison of experimental and theoretical results for concrete



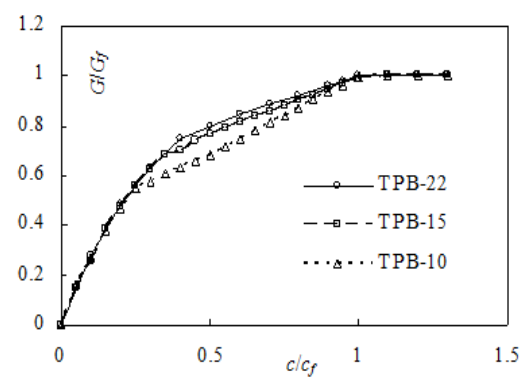
(a) $a_0=22\text{mm}$



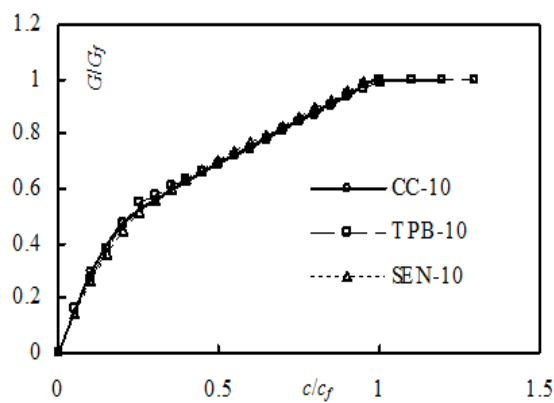
(a) CC



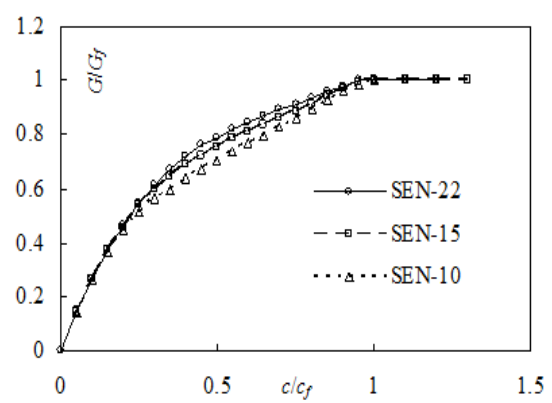
(b) $a_0=15\text{mm}$



(b) TPB



(c) $a_0=10\text{mm}$



(c) SEN

Fig. 7 R -curve dependence on geometry shape

Fig. 8 R -curve dependence on specimen size

$$\text{for SEN } \begin{cases} c_n = 1 \\ g_1(\alpha) = 0.265(1-\alpha)^4 + \frac{0.857+0.265\alpha}{(1-\alpha)^{3/2}} \end{cases} \quad (17)$$

Eq. (17) has an accuracy better than 1% for $\alpha < 0.2$, 0.5% for $\alpha \geq 0.2$.

$$\text{for CC } \begin{cases} c_n = 0.5 \\ g_1(\alpha) = \frac{1 - 0.5\alpha + 0.370\alpha^2 - 0.044\alpha^3}{\sqrt{1-\alpha}} \end{cases} \quad (18)$$

Eq.(18) has an accuracy of 0.3% for any α .

The R-curves for different geometries are shown in Fig.7. Interestingly, no apparent influence from geometry configuration is observed, which means for the same material with G_f and c_f as constants, TPB, SEN and CC specimen geometry share the same R-curve when the initial crack length a_0 keeps unvarying. While for different values of a_0 , R-curves exhibit obvious geometry-dependence in TPB, SEN and CC specimens as shown in Fig.8. For a shorter notch, less energy is needed for the same crack extension. Dimensionless geometry factor $g(a_0)$ and its derivative $g'(a_0)$ may be responsible for this behavior.

4. R-curve for type II and type III geometry

Type II geometry contains a fixed depth of specimen d and a varying a_0 , and this configuration is often used in laboratory to study material properties of fracture. When the basic Eq.(6) is used to deduce R-cure for type II, a_0 in the equation is treated as the parameter and $\partial G/\partial a_0$ is put to zero for every crack extension c , and by substituting a_0 into Eqs.(6)-(7a), one can easily get R-curve for a fixed value d . But one major disadvantage for one-size specimen is that an entire R-curve may not be achieved because of the limitation of specimen size, since c may not attain its peak value c_f because of no appropriate a_0 can be matched to this situation. But one deeper thought may be helpful. Bažant and his co-workers have identified that Eq.(3), the equation of the generalized SEL can be extended to variable-notch one-size test specimen, i.e., type II geometry. Consequently, the SEL-based R-curve proposed by Bažant for geometrically similar specimen (type III geometry) can be definitely regarded as R-curve for type II geometry. Next we use experimental data for concrete reported in (Tang *et al.*1996) to see how it works.

Batch 3 in (Tang *et al.*1996) had a mix proportion of 294:147:1134:756 of cement: water: coarse aggregate: sand by weight, and two series of beams were prepared: one is of geometrically similar beams with $a_0/d=0.4$ and d being 78.5mm, 115mm, 155mm and 230.5mm, the other was of the same size $d=152$ mm but different notches a_0/d being 0.25, 0.4 and 0.5. Both series had $s/d=2.5$. $G_f=0.0608$ N/mm and $c_f=22.5$ mm were evaluated from the first series specimen on the basis of SEL. By inserting $a_0/d=0.25, 0.4$ and 0.5 and $c_f=22.5$ mm into Eq.(6) and placing the partial derivative $\partial G/\partial d=0$, one can get a series of d values which constitutes the envelop of energy release rates for different specimen size. Then by combination with relation of Eqs.(7a)-(7b), R-curve for type III geometry is achieved. Fig.9 demonstrates the computation results. Note for specimen $s/d=2.5$, c_n and $g_1(\alpha)$ in Eq.(5) take the following form (Tang *et al.* 1996)

$$\begin{cases} c_n = 15/4 \\ g_1(\alpha) = \frac{1.83 - 1.65\alpha + 4.76\alpha^2 - 5.30\alpha^3 + 2.51\alpha^4}{\sqrt{\pi(1+2\alpha)(1-\alpha)^{3/2}}} \end{cases} \quad (19)$$

Eq. (19) is valid for $0.1 \leq \alpha \leq 0.6$.

For later usage, appropriate form must be sought to represent *R*-curve. Like in geometry type I, cubic function with respect to c/c_f is adopted here and the form is taken as Eq.(14). Table 4 lists the values of coefficients β_1 , β_2 , and β_3 introduced for a good regression.

Next we extend the *R*-curve determined above for type III geometry to type II geometry by comparing the predicted maximum stress with the experimental result. For crack begins to grow instable, the nominal stress reaches its maximum value and the energy release should fulfill two conditions represented by Eqs.(7a)-(7b). Substitute the expression of $G(a)$ and $R(c)$ decided above into Eqs.(7a)-(7b), we can get

$$G(a) = R(c) \Rightarrow \frac{\sigma_N^2 \pi a}{E} g_1^2(\alpha) = \left[\beta_1 \left(\frac{c}{c_f}\right)^3 + \beta_2 \left(\frac{c}{c_f}\right)^2 + \beta_3 \left(\frac{c}{c_f}\right) \right] G_f \quad (20a)$$

$$\frac{\partial G(a)}{\partial a} = \frac{\partial R(c)}{\partial c} \Rightarrow \frac{\sigma_N^2 \pi}{E} [g_1^2(\alpha) + 2\alpha g_1'(\alpha)] = \frac{G_f}{c_f} \left[3\beta_1 \left(\frac{c}{c_f}\right)^2 + 2\beta_2 \left(\frac{c}{c_f}\right) + \beta_3 \right] \quad (20b)$$

By means of Matlab software, the failure stress σ_N may be solved directly by eliminating c from Eqs.(20a)-(20b) and the results are listed in Table 5, and a great agreement is achieved.

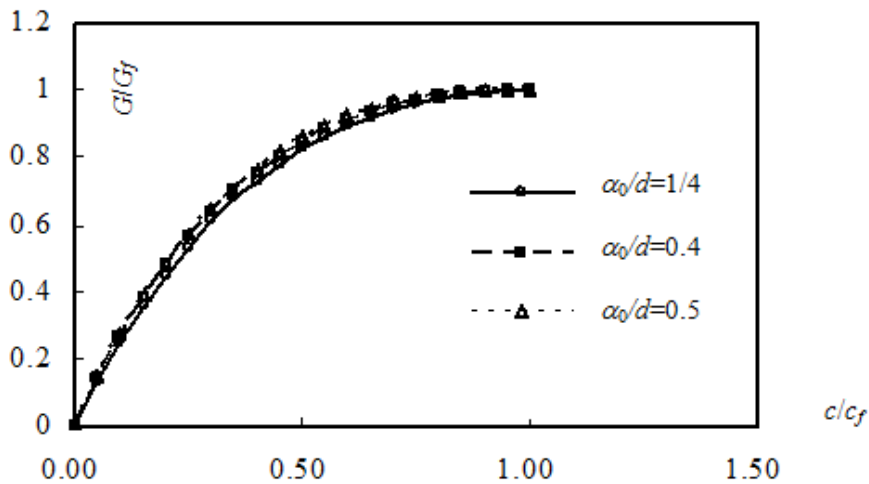


Fig.9 *R*-curve for type III with $c_f=22.5\text{mm}$

Table 4 β_1 , β_2 , and β_3 values for type III geometry with different a_0/d

a_0/d	β_1	β_2	β_3	R^2
0.25	0.8076	-2.5101	2.7025	0.9998
0.4	1.0106	-2.9083	2.8977	0.9997
0.5	0.9776	-2.9095	2.9319	0.9996

Table 5 Predicted values of σ_N and experimental results

$d(\text{mm})$	a_0/d	$\sigma_N(\text{MPa})$	
		Predicted results	Experimental results
152	0.25	2.899	2.767, 2.928(2.846)
	0.4	1.924	1.952, 1.967(1.959)
	0.5	1.375	1.302, 1,251(1.277)

* Note: value in the parenthesis is the average

5. Conclusions

G_f and c_f in the general SEL are believed to be material parameters and capable of constructing a simple *R*-curve model by defining *R*-curve as the envelope of the critical energy release rate of specimens of different sizes. *R*-curves for three typical geometries (type I, II and III) are provided using the general SEL, and much attention is paid to type I where the initial crack length a_0 keeps unchanged while the specimen depth d increases. Geometry type I is more of practical meaning when a_0 assumes to be a material's intrinsic property. The presented *R*-curve requires no measurements of crack length or compliance from the test. The study on type I shows the load-displacement response for quasi-brittle materials can well be described by the proposed *R*-curve approach and the *R*-curve for type I is strongly depended on a_0 but geometric shape has little influence on *R*-curve. In this sense, the *R*-curve may be said to be a material property. A special feature of the proposed *R*-curve is that crack resistance not only develops prior to the peak load but also in the post-peak regime. Also, *R*-curves originally determined for type III can be definitely applied to type II geometry.

Acknowledgements

The authors gratefully acknowledge the supports from National Basic Research Program of China (Grant No. 2015CB057703) and National Natural Science Foundation of China (Grant No. 51268010).

References

- Bazant, Z.P., Kim, J.K. and Pfeiffer, P.A. (1986), "Nonlinear fracture properties from size effect tests", *J. Struct. Eng. Div. ASCE*, **112**(2), 289-307.
- Bazant, Z.P. and Kazemi, M.T. (1990), "Determination of fracture energy, process zone length and brittle number from size effect with application to rock and concrete", *Int. J. Fract.*, **44**(2), 111-131.

- Bažant, Z.P., Gettu, R. and Kazemi, M.T. (1991), "Identification of nonlinear fracture properties from size effect tests and structural analysis based on geometry-dependent R-curves", *Int. J. Rock. Mech. Min.*, **28**(1), 43-51.
- de Moura, M.F.S.F., Morais, J.J.L. and Dourado, N. (2008), "A new data reduction scheme for mode I wood fracture characterization using the double cantilever beam test", *Eng. Fract. Mech.*, **75**(13), 3852-3865.
- de Moura, M.F.S.F., Dourado, N. and Morais, J.J.L. (2010), "Crack equivalent based method applied to wood fracture characterization using the single edge notched-three point bending test", *Eng. Fract. Mech.*, **77**(3), 510-520.
- Dong, W., Wu, Z.M. and Zhou, X.M. (2013), "Calculating crack extension resistance of concrete based on a new crack propagation criterion", *Constr. Build Mater.*, **38**, 879-889.
- Ferreira, L.E.T., Bittencourt, T.N., Sousa, J.L.A.O. and Gettu, R. (2002), "R-curve behavior in notched beam tests of rocks", *Eng. Fract. Mech.*, **69**(17), 1845-1852.
- Jenq, Y.S. and Shah, S.P. (1985a), "Two parameter fracture model for concrete", *J. Eng. Mech.*, **11**(10), 1227-1241.
- Jenq, Y.S. and Shah, S.P. (1985b), "A fracture toughness criterion for concrete", *Eng. Fract. Mech.*, **21**(5), 1055-1069.
- Krafft, J.M., Sullivan, A.M. and Boyle, R.W. (1961), "Effect of dimensions on fast fracture instability of notched sheets", Proceedings of the Crack Propagation Symposium, Cranfield, UK, August.
- Kumar, S. and Barai, S.V. (2009), "Weight function approach for determining crack extension resistance based on the cohesive stress distribution in concrete", *Eng. Fract. Mech.*, **76**, 1131-1148.
- Morel, S., Dourado, N., Valentin, G. and Morais, J. (2005), "Wood: a quasi-brittle material R-curve behavior and peak load evaluation", *Int. J. Fract.*, **131**(4), 385-400.
- Ouyang, C.S., Mobasher, B. and Shah, S.P. (1990), "An R-curve approach for fracture of quasi-brittle materials", *Eng. Fract. Mech.*, **37**(4), 901-913.
- Ouyang, C.S. and Shah, S.P. (1991), "Geometry-dependent R-curve for quasi-brittle materials", *J. Am. Ceram. Soc.*, **74**(11), 2831-2836.
- RILEM. (1990), "Determination of fracture parameters (K_{Ic} and $CTOD_c$) of plain concrete using Three-Point bend tests" (RILEM draft recommendations), *Mater. Struct.*, **23**(6), 457-460.
- RILEM. (1991), "Determination of the fracture energy of mortar and concrete by means of three-point bend tests on notched beams", *Mater. Struct.*, **18**(106), 285-290.
- Tada, H., Paris, P.C. and Irwin, G.R. (2000), The stress analysis of cracks handbook(Third Edition), The American Society of Mechanical Engineers ,Professional Engineering Publishing, New York, NY, USA.
- Tang, T.X., Bažant, Z.P., Yang, S. and Zollinger, D. (1996), "Variable-notch one-size test method for fracture energy and process zone length", *Eng. Fract. Mech.*, **55**(3), 383-404.
- Xu, S.L. and Zhang, X.F. (2008). "Determination of fracture parameters for crack propagation in concrete using an energy approach", *Eng. Fract. Mech.*, **75**, 4292-4308.
- Xu, F., Wu, Z.M., Zheng, J.J., Zhao, Y.H. and Liu, K. (2011), "Crack extension resistance curve of concrete considering variation of FPZ length", *J. Mater. Civil Eng. ASCE*, **23**, 703-710.
- Yang, W. and Shah, S.P. (2001), "A geometry and size dependent fracture resistance curve", *Int. J. Fract.*, **109**(3), 23-28.
- Zhao, Y.H., Xu, S.L. and Wu, Z.M. (2007), "Variation of fracture energy dissipation along evolving fracture process zones in concrete", *J. Mater. Civ. Eng.*, **19**(8), 625-633.